JOC Article

Computational Studies on Biosynthetic Carbocation Rearrangements Leading to Sativene, Cyclosativene, α-Ylangene, and β-Ylangene

Michael W. Lodewyk, Pradeep Gutta, and Dean J. Tantillo*

Department of Chemistry, University of California, Davis, One Shields Avenue, Davis, California 95616

tantillo@chem.ucdavis.edu

Received April 21, 2008

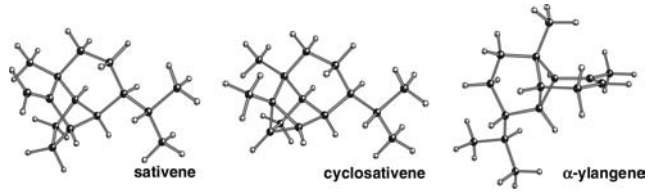

In this paper, we describe theoretical studies, using gas-phase quantum chemical calculations, on carbocationic rearrangement pathways leading to the sesquiterpenes sativene, cyclosativene, α-ylangene, and β-ylangene. For all four sesquiterpene natural products, viable pathways are presented, and these are compared both to mechanistic proposals found in the literature, and in certain cases to alternative stereochemical and rearrangement possibilities, thus providing a basis for comparison to experimental results. We find that these four sesquiterpenes likely arise from a common bicyclic intermediate and, furthermore, that the computed pathways are mostly in agreement with previous mechanistic proposals, although the few differences that we have uncovered are significant. Additionally, the potential energy profiles of the pathways are found to be very flat, supporting the notion that following the initial ionization of farnesyl diphosphate, minimal enzymatic intervention may be required for the generation of such sesquiterpenes.

Introduction

The ability of enzymes to construct an amazingly diverse array of complex natural products from a few simple precursors has intrigued chemists and biologists for decades. For example, the sesquiterpene synthase enzymes alone are known to produce hundreds of complex C_{15} hydrocarbons, which ultimately lead to thousands of richly functionalized natural products via derivatization by additional enzymes.[1] Remarkably, the substrate for all known sesquiterpene synthases is the same acyclic, achiral molecule—farnesyl diphosphate (FPP).[2–5]

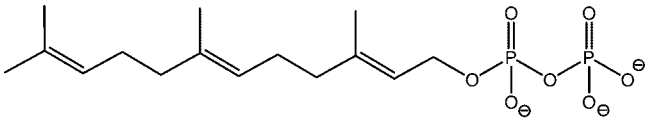

farnesyl diphosphate

It is often (but not always) a straightforward task to propose reasonable arrow-pushing mechanisms for the cationic rearrangements promoted by sesquiterpene synthases involving a series of simple intramolecular nucleophilic attacks on carbocationic centers; these include cyclizations, alkyl shifts, and hydride shifts. Such pathways often consist entirely of classical cationic species that interconvert via two-electron processes, although the intermediacy of nonclassical ions has been suggested in some cases.[6–8] In the course of our prior computational studies, we have uncovered evidence that unusual cations may

(1) *Encyclopedia of Terpenoids*; Glasby, J. S. Ed.; Wiley: Chichester, 1982.
(2) Christianson, D. W. *Chem. Rev.* **2006**, *106*, 3412–3442.
(3) Davis, E. M.; Croteau, R. *Top. Cur. Chem.* **2000**, *209*, 53–95.
(4) Cane, D. E. *Comp. Nat. Prod. Chem.* **1999**, *2*, 155–200.
(5) Cane, D. E. *Chem. Rev.* **1990**, *90*, 1089–1103.

(6) For leading references on nonclassical carbocations, see: (a) Grob, C. A. *Acc. Chem. Res.* **1983**, *16*, 426–431. (b) Brown, H. C. *Acc. Chem. Res.* **1983**, *16*, 432–440. (c) Olah, G. A.; Prakash, G. K. S.; Saunders, M. *Acc. Chem. Res.* **1983**, *16*, 440–448. (d) Walling, C. *Acc. Chem. Res.* **1983**, *16*, 448–454. (e) Brown, H. C. (with comments by P. v. R. Schleyer). *The Nonclassical Ion Problem*; Plenum: New York, 1977.

(7) Nonclassical cations have, from time to time, been proposed as intermediates in terpene biosynthesis. See, for example: (a) Wessjohann, L. A.; Brandt, W. *Chem. Rev* **2003**, *103*, 1625–1647. (b) Giner, J.-L.; Buzek, P.; Schleyer, P. v. R. *J. Am. Chem. Soc.* **1995**, *117*, 12871–12872. (c) Erickson, H. K.; Poulter, C. D. *J. Am. Chem. Soc.* **2003**, *125*, 6886–6888. (d) He, X.; Cane, D. E. *J. Am. Chem. Soc.* **2004**, *126*, 2678–2679. (e) Dewar, M. J. S.; Ruiz, J. M. *Tetrahedron* **1987**, *43*, 2661–2674. (f) Olah, G. A. *Angew. Chem., Int. Ed. Engl.* **1995**, *34*, 1393–1405.

(8) For leading references to older proposals by Djerassi, Arigoni, and Eschenmoser, see: Giner, J.-L. *Chem. Res.* **1993**, *93*, 1735–1752.

10.1021/jo800868r CCC: $40.75
Published on Web 08/06/2008

SCHEME 1

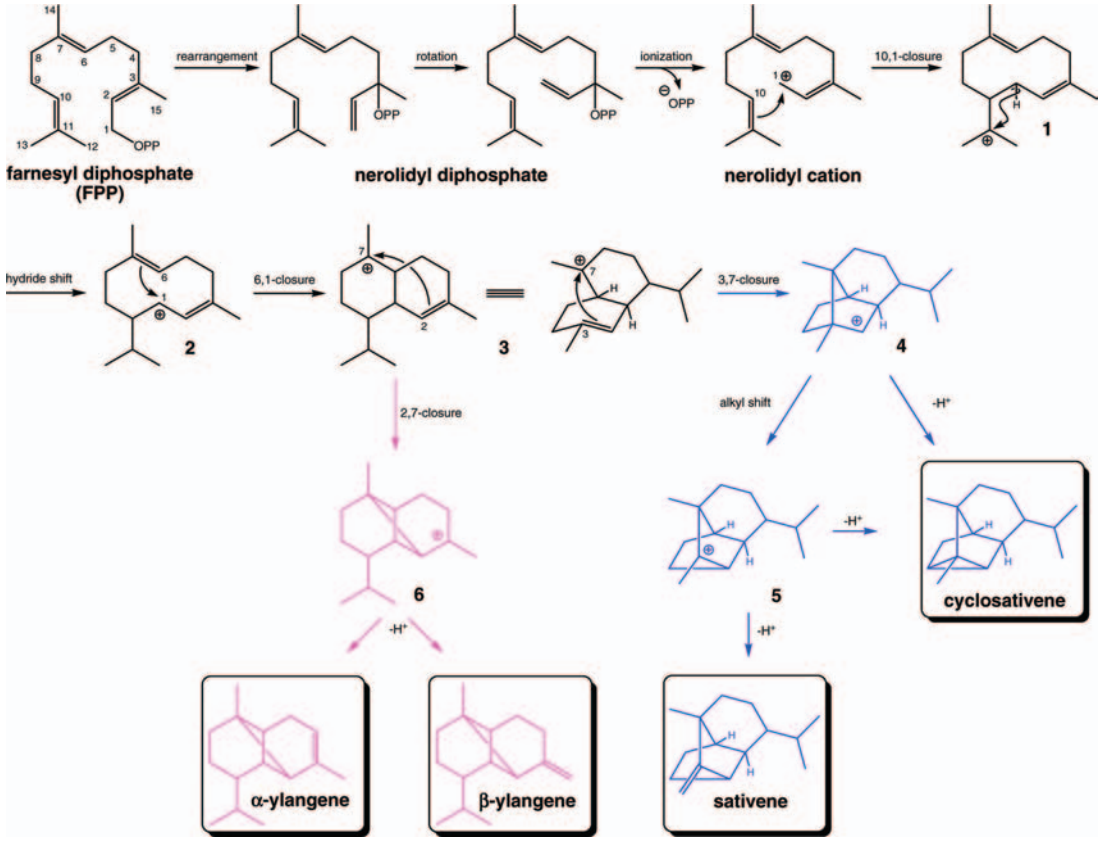

indeed play key roles in sesquiterpene-forming rearrangements.[9–16] For example, in some cases, the formation of especially reactive species such as secondary carbocations appears to be avoided altogether through the combination of simple two-electron reactions into concerted processes.[12,17] Even in less extreme cases, many of the carbocations we have characterized computationally benefit from intramolecular stabilization in the form of strong hyperconjugation, cation$-\pi$ interactions, and delocalization via bridging to form nonclassical (i.e., carbonium) ions.[9–15] Although these sorts of internal (intramolecular) stabilization may be replaced by external (intermolecular) stabilization provided by the enzyme in which the carbocations are generated, we feel that it is still of great utility to explore the inherent reactivity of these species. In part, this is because at times it has been suggested that the role of the terpene synthase enzymes is mainly to facilitate the initial ionization of the diphosphate group, and then to provide a protective environment (from outside nucleophilic attack) and some conformational guidance to the carbocationic intermediates.[18] Indeed, we often find that even in gas-phase calculations, the barriers associated with carbocationic rearrangements in sesquiterpene formation are small.[10–12] When certain steps do appear to have relatively high barriers, our gas-phase studies provide a starting point for examining just how the enzyme might intervene.[12] In short, modern computational chemistry techniques can provide invaluable insight into the mechanistic details of sesquiterpene formation.

Many terpene synthase enzymes demonstrate high selectivity, making predominantly only one product,[2–5] while others lack this fidelity and generate numerous terpene products.[19–23] One enzyme of the latter type, γ-humulene synthase isolated from the Grand Fir (*Abies grandis*), has been reported to produce

(9) Hong, Y. J.; Tantillo, D. J. *J. Org. Chem.* **2007**, *72*, 8877–8881.
(10) Gutta, P.; Tantillo, D. J. *Org. Lett.* **2007**, *9*, 1069–1071.
(11) Hong, Y. J.; Tantillo, D. J. *Org. Lett.* **2006**, *8*, 4601–4604.
(12) Gutta, P.; Tantillo, D. J. *J. Am. Chem. Soc.* **2006**, *128*, 6172–6179.
(13) Ponec, R.; Bultinck, P.; Gutta, P.; Tantillo, D. J. *J. Phys. Chem. A* **2006**, *110*, 3785–3789.
(14) (a) Bojin, M. D.; Tantillo, D. J. *J. Phys. Chem. A* **2006**, *110*, 4810–4816. (b) Most prominent among the candidates for active-site bases in terpene synthases are histidine residues and departed pyrophosphate.[1–5] Ammonia was used in our calculations (see also refs 9 and 14a) for simplicity. Reference 9 demonstrates that interaction with the lone pair of ammonia or a π-face of benzene leads to qualitatively similar perturbations to carbocation structure, despite their very different basicities and electronic structures. Nonetheless, our ongoing studies will address more quantitatively the implications of using different model bases on such processes; results along these lines will be reported in due course.
(15) Gutta, P.; Tantillo, D. J. *Angew. Chem., Int. Ed.* **2005**, *44*, 2719–2723.
(16) Additional calculations on cation rearrangements in sesquiterpene biosynthesis have been described by Allemann, Gao, Truhlar, and co-workers; see: Allemann, R. K.; Young, N. J.; Ma, S.; Truhlar, D. G.; Gao, J. *J. Am. Chem. Soc.* **2007**, *129*, 13008–13013.
(17) Hong, Y. J.; Wang, S. C.; Tantillo, D. J. Unpublished results.
(18) Kinetic studies on certain sesquiterpene synthases have suggested that the initial divalent metal ion-dependent ionization of the pyrophosphate group may be the rate-limiting chemical step in terpene formation; see: (a) Cane, D. E.; Chiu, H.-T.; Liang, P.-H.; Anderson, K. S. *Biochemistry* **1997**, *36*, 8332–8339. (b) Mathis, J. R.; Back, K.; Starks, C.; Noel, J.; Poulter, C. D.; Chappell, J. *Biochemistry* **1997**, *36*, 8340–8348.
(19) (a) Little, D. B.; Croteau, R. B. *Arch. Biochem. Biophys.* **2002**, *402*, 120–135. (b) Steele, C. L.; Crock, J.; Bohlmann, J.; Croteau, R. *J. Biol. Chem.* **1998**, *273*, 2078–2089.
(20) δ-Selinene synthase is another such "promiscuous" enzyme, making approximately 30 different sesquiterpenes, including α-ylangene as a minor product (see ref 19).
(21) For an example of such a case with a triterpene synthase, see: Lodeiro, S.; Xiong, Q.; Wilson, W. K.; Kolesnikova, M. D.; Onak, C. S.; Matsuda, S. P. T. *J. Am. Chem. Soc.* **2007**, *129*, 11213–11222.
(22) Yoshikuni, Y.; Ferrin, T. E.; Keasling, J. D. *Nature* **2006**, *440*, 1078–1082.
(23) Cane, D. E. *Nat. Chem. Biol.* **2006**, *2*, 179–180.

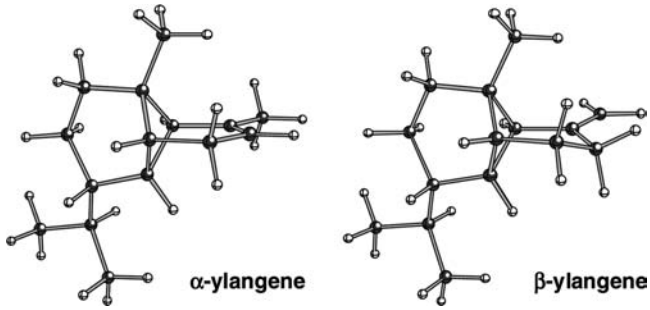

FIGURE 1. Ball & Stick representation of the two ylangene structures (B3LYP/6-31+G(d,p) level of theory).

over 50 known sesquiterpenes.[19] Among the sesquiterpenes produced by this enzyme are sativene,[24] cyclosativene,[25] α-ylangene, and *β*-ylangene[26] (Scheme 1). These four sesquiterpenes are proposed to occur along a common thread in terpene biosynthesis, originating from the 10,1-closure of nerolidyl diphosphate as shown in Scheme 1.[19,20,27,28] Sativene and cyclosativene contain complex ring systems derived from a bornyl-type intermediate that is often formulated as a secondary carbocation (**4**), which one might expect to be a relatively high energy intermediate.[6,17] The two ylangenes feature an interesting ring system consisting of a central four-membered ring with two six-membered rings bridging its faces and oriented orthogonally to each other. These features are not readily apparent in the structures drawn in Scheme 1, but they are revealed quite clearly in the three-dimensional pictures shown in Figure 1. Additionally, the proposed pathway to the ylangenes involves the formation of a tertiary carbocation directly adjacent to their central four-membered ring (**6**, Scheme 1). Similar to the secondary carbocation mentioned above, this sort of system might be expected to be relatively high in energy and may not exist as a minimum.[29–31] These features led to our interest in this particular segment of sesquiterpene biosynthesis. In this paper, we examine the detailed pathways specifically leading to sativene, cyclosativene, and the ylangenes.[32]

Methods

All calculations were performed with the Gaussian03[33] software suite. Geometries were optimized without symmetry constraints using the B3LYP/6-31+G(d,p) method.[34] All stationary points were characterized as either minima or transition-state structures via frequency calculations, and the reported energies include unscaled zero-point energy (ZPE) corrections. For every reaction step except one,[35] the transition-state structures were linked to their corresponding minima via intrinsic reaction coordinate (IRC)[36] calculations. Structural diagrams were produced using Ball & Stick version 4.0.[37]

In prior work on mechanisms of sesquiterpene biosynthesis, we have utilized the B3LYP/6-31+G(d,p) method and have discussed the general applicability of this method to the sorts of transformations involved in complex carbocation rearrangements.[9–15] However, a recent report suggests that the B3LYP method systematically underestimates the exothermicity of cyclization reactions and recommends the use of mPW1PW91 single-point energies with B3LYP-optimized geometries.[38] Accordingly, single-point calculations at the mPW1PW91/6-31+G(d,p)//B3LYP/6-31+G(d,p) level were performed on all stationary point structures involved in the major pathways.[11,12] The energies reported here include unscaled ZPE corrections derived from the B3LYP frequency calculations.

Results and Discussion

Sativene. The proposed pathway[19,20] to sativene is shown in Scheme 1. This mechanism includes initial ionization and rearrangement of FPP to produce cisoid nerolidyl diphosphate, which then undergoes a second ionization to produce the nerolidyl cation, a common and necessary feature of many biosynthetic transformations leading to sesquiterpenes harboring cis double bonds or formed from intermediates with cis double bonds.[2–5] The pathway then continues with a typical series of ring-closure and hydride/alkyl shift steps before the cascade is terminated by a final deprotonation step that results in sativene. Importantly, while Scheme 1, as reported in ref 19, does not explicitly show many stereochemical details, Arigoni et al. have reported the results of extensive labeling experiments which provide valuable insight into the biosynthesis of (−)-sativene (from *Helminthosporium victoriae* and *Helminthosporium sa-*

(24) de Mayo, P.; Williams, R. E. *J. Am. Chem. Soc.* **1965**, *87*, 3275.
(25) Smedman, L.; Zavarin, E. *Tetrahedron Lett.* **1968**, *35*, 3833–3835.
(26) (a) Hunter, G. L. K.; Veldhuis, M. K. *J. Food Sci.* **1967**, *32*, 697. (b) Motl, O.; Bucharov, V. G.; Šorm, F. *Chem. Ind.* **1963**, *44*, 1759–1760. (c) Hunter, G. L. K.; Brogden, W. B., Jr. *J. Org. Chem.* **1964**, *29*, 982–983, and references therein. (d) For a recent report of α-ylangene isolated from a marine diterpene synthase, see: Brück, T. B.; Kerr, R. G. *Comp. Biochem. Physiol., Part B: Biochem. Mol. Biol.* **2006**, *143*, 269–278.
(27) Schemes found in ref 19 also include *β*-cubebene (found as a minor product of *γ*-humulene synthase and proposed to arise from a 1,2-hydride shift in intermediate **3**, Scheme 1) and α-copaene (a diastereomer of α-ylangene found as a minor product of both *γ*-humulene synthase and *δ*-selinene synthase). However, we find that the relative stereochemistry in structure **3** that leads to sativene, cyclosativene, and the ylangenes is not consistent with the relative stereochemistry of *β*-cubebene and α-copaene. Therefore, we believe that *β*-cubebene and α-copaene do not arise directly from intermediate **3**, but rather may arise via an earlier branch point. See the Supporting Information for a scheme which illustrates this relationship. Additionally, according to ref 19, there are several other sesquiterpenes which may arise from deprotonation−reprotonation sequences along the way to sativene, etc. (e.g. germacrenes, amorphenes, sibirene, and gurjunene); these are not discussed further in this manuscript.
(28) While sativene, cyclosativene, α-ylangene, and *β*-ylangene are found as constituents of numerous natural product extracts, to our knowledge, only one, *β*-ylangene, has been linked to another known sesquiterpene synthase enzyme, namely germacrene D synthase. See: Deguerry, F.; Pastore, L.; Wu, S.; Clark, A.; Chappell, J.; Schalk, M. *Arch. Biochem. Biophys.* **2006**, *454*, 123–136.
(29) Reddy, V. P.; Rasul, G.; Prakash, G. K. S.; Olah, G. *J. Org. Chem.* **2007**, *72*, 3076–3080.
(30) Siehl, H.-U. *Chem. Cyclobutanes* **2005**, *1*, 521–547.
(31) For a review on related cyclopropylcarbinyl cations, see: Olah, G. A.; Reddy, P.; Prakash, G. K. S. *Chem. Rev.* **1992**, *92*, 69–95.
(32) This report is part three in our "Theoretical Studies on Farnesyl Cation Cyclization" series in which we explore the mechanistic details of sesquiterpene formation using quantum mechanical calculations. For parts 1 and 2, see refs 11 and 12.
(33) Frisch, M. J. *Gaussian03, revision D.01*; Gaussian, Inc.: Pittsburgh, PA, 2003 (see the full reference in the Supporting Information).
(34) (a) Becke, A. D. *J. Chem. Phys.* **1993**, *98*, 5648–5652. (b) Becke, A. D. *J. Chem. Phys.* **1993**, *98*, 1372–1377. (c) Lee, C.; Yang, W.; Parr, R. G. *Phys. Rev. B* **1988**, *37*, 785–789. (d) Stephens, P. J.; Devlin, F. J.; Chabalowski, C. F.; Frisch, M. J. *J. Phys. Chem.* **1994**, *98*, 11623–11627. (e) The value of diffuse functions in density functional based calculations was recently discussed in: Lynch, B. J.; Zhao, Y.; Truhlar, D. G. *J. Phys. Chem. A* **2003**, *107*, 1384–1388.
(35) We were unable to complete an IRC calculation linking transition structure **TS3c→6** to minimum **6** (Figure 8). While the vibrational mode corresponding to the imaginary frequency associated with the transition structure clearly shows motion corresponding to the expected bond formation, the flat nature of the potential energy surface appears to prevent the IRC calculation from effectively following the surface towards intermediate **6**.
(36) (a) Gonzalez, C.; Schlegel, H. B. *J. Phys. Chem.* **1990**, *94*, 5523–5527. (b) Fukui, K. *Acc. Chem. Res.* **1981**, *14*, 363–368. (c) IRC plots are available in the Supporting Information.
(37) Müller, N.; Falk, A.; Gsaller, G. *Ball & Stick V.4.0a12, molecular graphics application for MacOS computers*; Johannes Kepler University: Linz, 2004.
(38) Matsuda, S. P. T.; Wilson, W. K.; Xiong, Q. *Org. Biomol. Chem.* **2006**, *4*, 530–543.
(39) (a) Arigoni, D. *Pure Appl. Chem.* **1975**, *41*, 219–245. (b) Dorn, F.; Bernasconi, P.; Arigoni, D. *Chimia* **1975**, *29*, 24–25. (c) Cane, D. E. In *Biosynthesis of Isoprenoid Compounds*; Porter, J. W., Spurgeon, S. L. Eds.; Wiley: New York, 1981; Vol. 1, Chapter 6.

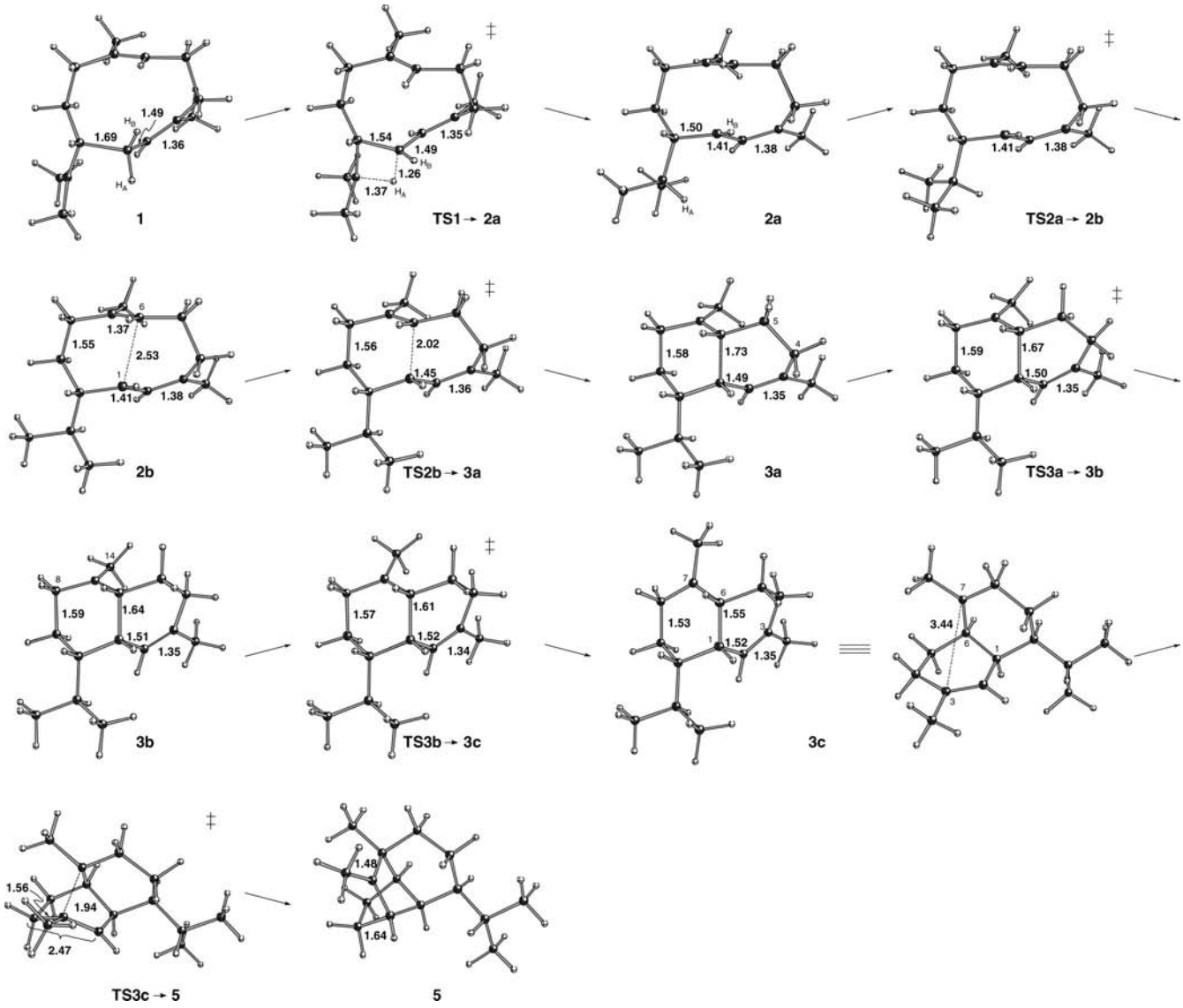

FIGURE 2. Computed geometries (B3LYP/6-31+G(d,p), selected distances in Å) for structures involved in the transformation of **1** to **5** in Scheme 1. See Scheme 2 for corresponding mechanistic steps.

tivum).[39] Although γ-humulene synthase (from *A. grandis*) is known to produce the enantiomeric (+)-sativene,[40] the results from the labeling studies for (−)-sativene are relevant in their implications for the relative stereochemistry of sativene and will be discussed in conjunction with the results presented herein.

We began our calculations with the 10,1-closure intermediate (**1**), since the appropriately folded nerolidyl cation structure could not be found as a minimum.[41] Our calculated pathway is shown in Figure 2, and the corresponding mechanistic steps are depicted in Scheme 2. Figure 3 shows the relative energies (B3LYP and mPW1PW91) for the stationary points shown in Figure 2. From **1** in Figure 2, a 1,3-hydride shift occurs (to form **2a**), followed by a conformational change involving the isopropyl group (**2a** → **2b**).[42] The hydride shift illustrated by **TS1**→**2a** in Figure 2 specifically involves H_A (one of two diastereotopic hydrogen atoms on C1; the one which is syn to the isopropyl group). Migration of this hydrogen leads to the correct relative stereochemistry of sativene, consistent with the reported labeling studies.[39] The corresponding shift of H_B (anti to the isopropyl group) would instead lead toward a different, but related, mechanistic pathway: one which apparently does not occur in γ-humulene synthase.[19] Although exploration of this pathway is beyond the scope of this report, preliminary calculations suggest that the shift of H_B would occur through a transition-state structure that is approximately 5 kcal/mol higher in energy than the transition-state structure corresponding to

(40) (a) Smedman, L. A.; Zavarin, E.; Teranishi, R. *Phytochemistry* **1969**, *8*, 1457–1470. (b) Smedman, L. A.; Snajberk, K.; Zavarin, E.; Mon, T. R. *Phytochemistry* **1969**, *8*, 1471–1479.

(41) Attempts to find an open form of the nerolidyl cation in a productive conformation repeatedly led either directly to structure **1** or to the bisabolyl cation. Our attempts included the use of both constrained calculations and relaxed potential energy surface scans involving the C1−C10 distance.

(42) (a) Although rotation of the isopropyl group at this point is not essential for the ultimate formation of sativene, cyclosativene, and the ylangenes, it does result in an overall lower energy pathway. See the Supporting Information for structures and energies corresponding to the pathway leading to sativene without this early conformational change. (b) The conformation of the isopropyl group also appears to perturb the potential energy surface in the region of the **3c**→**5** and **3c**→**6** reaction steps. Specifically, whereas the IRC results pictured in Figure 4 smoothly connect **TS3c**→**5** to intermediate **3c** in the reverse direction, the corresponding IRC result for **TS3c′**→**5′** (where the isopropyl group is in its **2a** conformation) appears to lead directly to **TS3c′**→**6′**, a transition-state structure leading to the ylangene cation; this feature is most likely indicative of a bifurcation along this pathway. See the Supporting Information for diagrams and additional details.

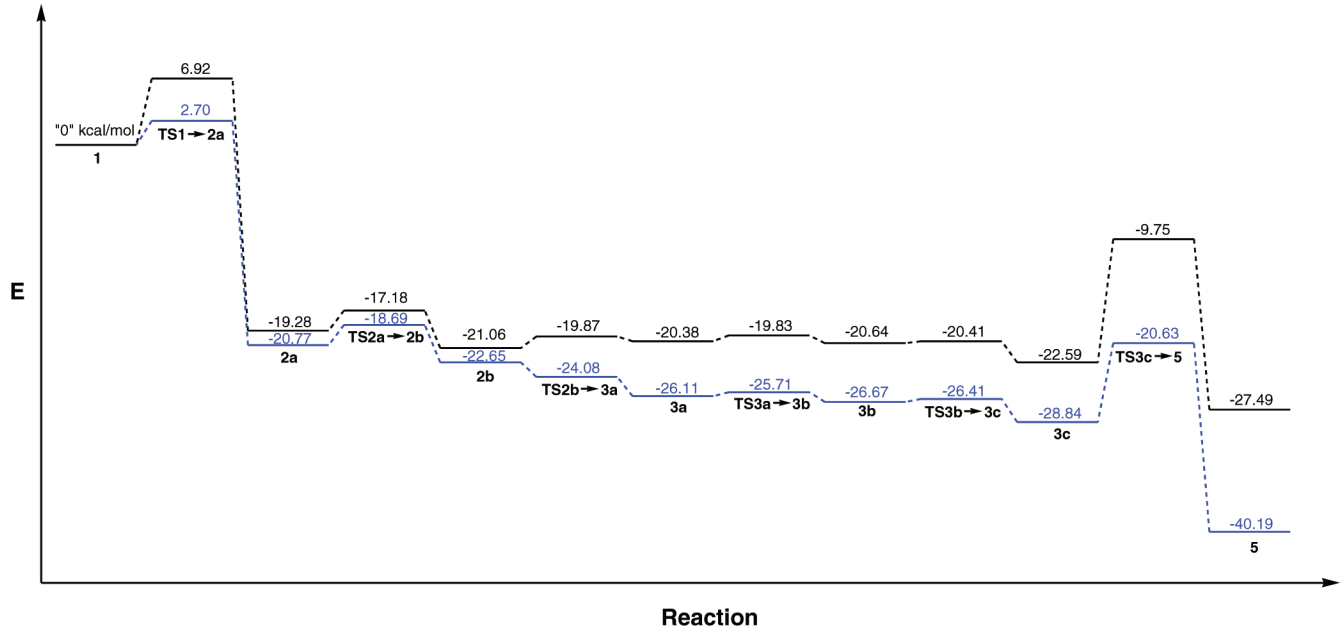

FIGURE 3. Relative energy diagram corresponding to the computed pathway shown in Figure 2. Bold numbers under each horizontal line correspond to the structure numbers in Figure 2. All energies are in kcal/mol and are expressed relative to structure **1**. The black lines and numbers represent energies calculated with B3LYP/6-31+G(d,p), and the blue lines and numbers represent energies calculated with mPW1PW91/6-31+G(d,p)// B3LYP/6-31+G(d,p) (zero-point energy corrections from B3LYP calculations included in the mPW1PW91 energies).

SCHEME 2

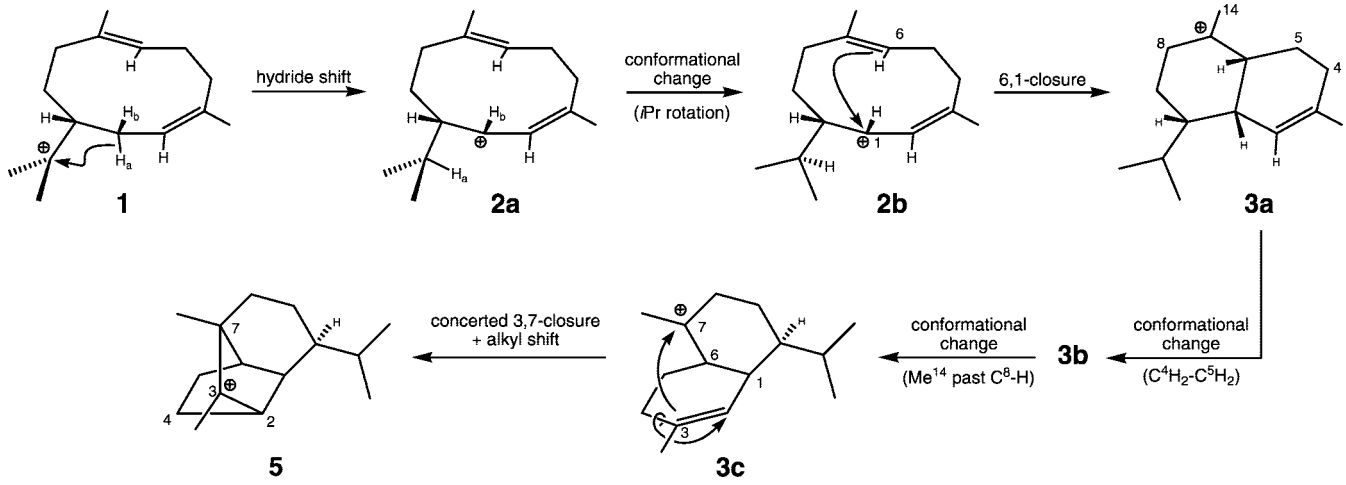

the shift of H_A. Thus it is not surprising that a sativene-forming enzyme is able to differentiate between these two pathways.[43] In all, the transformation from **1** to **2b** is exothermic by approximately 21−23 kcal/mol, resulting in part from the conversion of a tertiary carbocation to one that is both tertiary and allylic.[44]

The resulting carbocation (**2b**) then undergoes 6,1-closure to produce a bicyclic ring system with a tertiary carbocation center (**3a**) in a step that is predicted to be exothermic by 3.5 kcal/mol by mPW1PW91 and slightly endothermic by the B3LYP method. With either method, the barrier for this step is very small, consistent with the fact that little geometric change is required for this attack to occur. In fact, with a distance of 2.53 Å between the allylic carbocation and the π-bonded carbon, the intramolecular cation−π interaction[45] in **2b** is on the verge of bond formation and very nearly makes this reaction step barrierless. From this point, two conformational changes are required to prepare the substrate for the next ring closure. The first of these involves an internal rotation about the C4−C5 single bond in the cyclohexene ring of approximately 70 degrees, resulting in a boat → half-chair conformational change for this

(43) Note that the presence of a direct 1,3-hydride shift pathway from **1** to **2**, even though it is energetically feasible, does not rule out the possibility of alternative deprotonation-reprotonation sequences involving a bicyclogermacrene intermediate, as suggested by Cane and co-workers in work on related rearrangements; see: Jiang, J.; Cane, D. E. *J. Am. Chem. Soc.* **2008**, *130*, 428–429. See also ref 7d for a paper on germacrene D. Note that it is difficult to assess the energetics of such intermolecular alternatives.

(44) Lossing, F. P.; Holmes, J. L. *J. Am. Chem. Soc.* **1984**, *106*, 6917–6920.

(45) Computations on complexes of classical cations with π-systems include: (a) Miklis, P. C.; Ditchfield, R.; Spencer, T. A. *J. Am. Chem. Soc.* **1998**, *120*, 10482–10489. (b) Filippi, A.; Roselli, G.; Renzi, G.; Grandinetti, F.; Speranza, M. *Chem.—Eur. J.* **2003**, *9*, 2072–2078. (c) Berthomieu, D.; Brenner, V.; Ohanessian, G.; Denbez, J. P.; Millié, P.; Audier, H. E. *J. Phys. Chem.* **1995**, *99*, 712–720. (d) Chalk, A. J.; Radom, L. *Int. J. Mass Spectrom.* **2000**, *199*, 29–40. (e) Heidrich, D. *Angew. Chem., Int. Ed.* **2002**, *41*, 3208–3210. (f) Marcantoni, E.; Roselli, G.; Lucarelli, L.; Renzi, G.; Filippi, A.; Trionfetti, C.; Speranza, M. *J. Org. Chem.* **2005**, *70*, 4133–4141. (h) Jenson, C.; Jorgensen, W. L. *J. Am. Chem. Soc.* **1997**, *119*, 10846–10854.

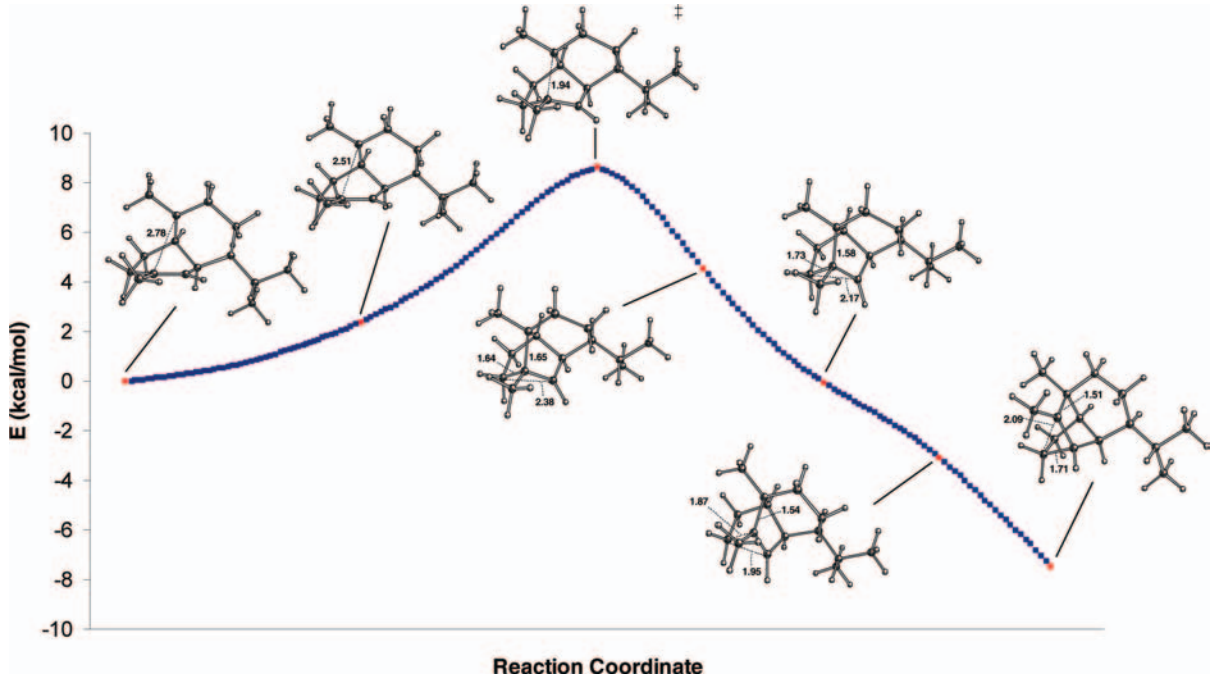

FIGURE 4. IRC diagram representing the computed potential energy surface for the conversion of structure **3c** to **5** in Figure 2. The highest energy structure shown is that of the transition state (**TS3c→5**). The first and last structures correspond to the terminal points in the IRC calculation. The corresponding minima (**3c** and **5**) are shown in Figure 2.The red dots indicate which points are represented by the structures.

ring (**3a** → **3b**). Next, the methyl group (C14) connected to the carbocation must move past the neighboring C8−H bond (**3b** → **3c**).[46] While the first conformational change is roughly degenerate energetically, the second is exothermic by approximately 2 kcal/mol. The resulting structure (**3c,** see Figure 2 and Scheme 2) shows a decrease in the C1−C6 bond distance, which reflects a decrease in hyperconjugation with the carbocationic center (for the C1−C6 σ bond), but likely reduces the overall ring strain of the system.

Up to this point, with the inclusion of the three conformational changes, our computed pathway is fully consistent with the proposed pathway shown in Scheme 1. The next step in the proposal involves a 3,7-ring closure to produce a secondary carbocation (**4**). An attempt to find a transition-state structure for this transformation resulted in structure **TS3c→5** in Figure 2. Examination of the vibrational mode corresponding to the imaginary frequency associated with this structure left little doubt that it is in fact the transition structure for cyclization. However, completion of an IRC calculation revealed that the structure was actually connected to the cation (**5**) immediately preceding sativene. As shown in Figure 4, the IRC in the forward direction suggests that the secondary cation is not a minimum and that the subsequent alkyl shift occurs along with ring-closure in a concerted reaction, with the two steps occurring asynchronously.[47,48] The asynchronicity of these two steps is further illustrated in Figure 5, which shows that C3−C7 bond formation precedes the alkyl shift (and associated C2−C4 bond formation). Additionally, explicit attempts to find the proposed secondary cation as a minimum failed.[49] These results are consistent with our observation in other sesquiterpene pathways in that we rarely find secondary cations as minima.[11,17] Structure **5** in Figure 2 is the cation immediately preceding sativene; deprotonation at the C15 methyl group will produce the final sesquiterpene product.

The energetic changes associated with sativene formation are shown in Figure 3. As expected,[38] the mPW1PW91 energy profile shows an overall greater exothermicity than the B3LYP profile. This difference in energetics does not significantly change the mechanistic picture, however. Between the first and last steps, which have the highest barriers (and are also the most exothermic), the pathway is extremely flat, with several nearly barrierless steps that are comprised of conformational changes and one cyclization. Even the barrier associated with the final step, which is the largest among the barriers for the individual steps in the rearrangement, has a computed range of only 8−13 kcal/mol. Altogether, these results can be taken as support of the proposal that minimal enzymatic intervention—specifically in terms of reducing activation barriers—is required to form sativene once the pyrophosphate group has been detached.

As a side point, the possibility of sativene formation via a crossover from the copacamphene (a diastereomer of sativene) pathway to the sativene pathway (and vice versa) via a 1,2-shift of the C8−C9 bridge in **5** has previously been put forth in the literature, although labeling experiments indicate that this does not occur in the biosynthesis of (−)-sativene.[39a] As illustrated in Figure 6, we were able to find a transition-state structure for this rearrangement. This structure is connected on

(46) Structures **3b** and **3c** can be considered to be hyperconjomers: Rauk, A.; Sorensen, T. S.; Schleyer, P. v. R. *J. Chem. Soc. Perkin Trans. 2* **2001**, *6*, 869–874. In **3b**, the cation is hyperconjugated to two neighboring C-C sigma bonds, while in **3c**, the cation is hyperconjugated to two neighboring C−H σ bonds.

(47) If the C15 methyl group were to be absent, then the alkyl shift would result in an alternative secondary carbocation. Interestingly, an IRC calculation on such a structure also shows the alkyl shift to occur in a concerted fashion along with the ring closure. Optimization of the resulting minimum results in a bridged, nonclassical carbonium ion species. See the Supporting Information for the IRC and associated minimum.

(48) Tantillo, D. J. *J. Phys. Org. Chem.* **2008**, *21*, 561–570.

(49) These attempts included the use of constrained optimizations (in order to prevent the alkyl shift from occurring) both on structures similar to the transition state structure (Figure 4) and on structures with ammonia complexed to several nearby hydrogen atoms. In all cases, when the constraint was removed, the structure relaxed to one corresponding to structure **5** (Figure 2).

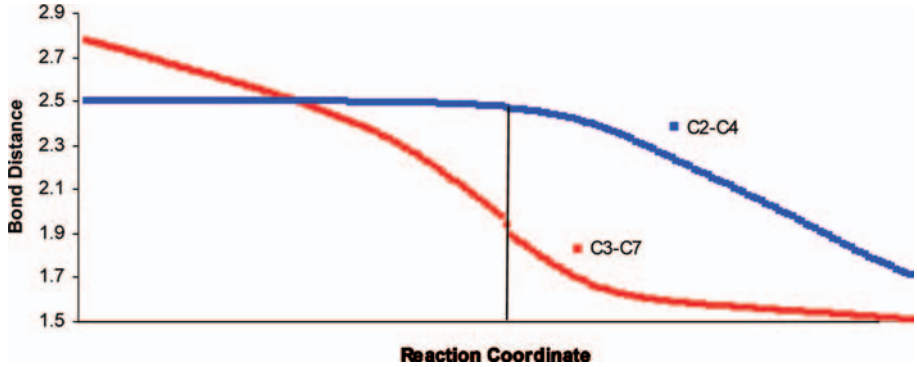

FIGURE 5. Plot illustrating the asynchronous nature of the 3,7-closure and alkyl shift reaction steps in the concerted reaction **3c** → **5**. The bond distance coordinate is in Å, and the vertical line marks the point of the transition-state structure. At this point, the C3−C7 bond corresponding to the ring-closing step has clearly begun to form, while the C2−C4 distance corresponding to the alkyl shift remains largely unchanged until later along the reaction coordinate.

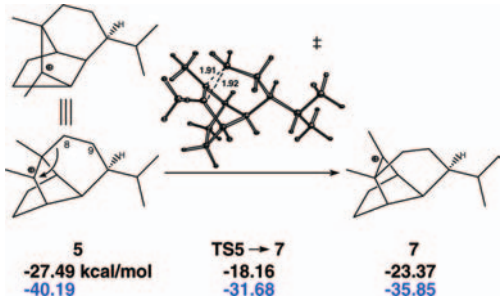

FIGURE 6. Computed geometry and energies for structures involved in the transformation of the sativene precursor (**5**) to the copacamphene precursor (**7**). Energies are in kcal/mol and are relative to that of structure **1**; selected distances are in Å. Distances and energies shown in black are calculated with B3LYP/6-31+G(d,p) and energies shown in blue are calculated with mPW1PW91/6−31+G(d,p)//B3LYP/6−31+G(d,p) (zero-point energy corrections from B3LYP calculations are included in the mPW1PW91 energies).

one side to structure **5**, the immediate precursor to sativene, and on the other side to **7**, the immediate precursor to copacamphene. Our calculations suggest that this rearrangement could occur with a barrier of approximately 9 kcal/mol (from **5**). The apparent absence of copacamphene products from γ-humulene synthase,[19] however, suggests that this step might require enzymatic intervention (either in selectively accelerating the rearrangement or perhaps in discouraging the deprotonation leading to sativene and cyclosativene), that γ-humulene synthase[19] (or the sativene-forming enzymes in *H. victoriae* and *H. sativum*[24,39]) does not offer.

Cyclosativene. As shown in Scheme 1, there are at least two potential routes to cyclosativene—both involving deprotonation/ring-closure steps from intermediates proposed in the pathway to sativene (**4** and **5**). Note, however, that one of these two routes involves the secondary carbocation (**4**) that we were unable to locate computationally. Therefore, we propose that (at least in the absence of the enzyme) the only route to cyclosativene is through **5**, the cation immediately preceding sativene. In order to test whether the deprotonation/ring-closing step required to make cyclosativene is feasible for this intermediate, we sought a transition state structure for this sort of transformation. Since we have no explicit knowledge regarding the identity of the active site base that could be responsible for the deprotonation, we chose ammonia as a representative base (which can be considered to be a crude mimic of a lysine side chain).[9,14] The resulting transition-state structure (**8**) is shown in Figure 7, along with the corresponding exo and endo transition-state structures (**9** and **10**)[50] for deprotonation of **5** to form sativene for comparison.[51] An attempt to find a transition-state structure for deprotonation of H_D in **8** led to structure **9**. Note that although it is a transition structure, **8** actually resembles a nonclassical carbonium ion.[6] An IRC plot and the imaginary frequency associated with **8** confirm that it is indeed a transition structure for the formation of cyclosativene. Therefore, we conclude that this type of deprotonation/ring-closure reaction—from **5**, not **4**—is a viable means of forming cyclosativene.

α-Ylangene and β-Ylangene.[52] The proposed branch point for the formation of the two ylangenes is structure **3** in Scheme 1; an alternative 2,7-ring closure here would produce structure **6**, the immediate precursor to the ylangenes. As shown in Figure 8, we were able to find a transition-state structure (**TS3c→6**) for this cyclization. An IRC calculation revealed that this transition-state structure follows structure **3c**,[42b] which is also the conformer of the bicyclic ring system that immediately precedes the concerted ring closure + alkyl shift leading to the sativene/cyclosativene cation **5** (Figure 2). The barrier for ring-closure through **TS3c→6** is approximately 1−4 kcal/mol—significantly lower than the barrier leading toward sativene and cyclosativene. This may be a bit surprising considering that this step forms a strained, four-membered ring. However, it also transforms one tertiary carbocation into another, while the transition-state structure leading to the sativene/cyclosativene cation (**TS3c→5**) displays secondary carbocationic character (the asynchronous alkyl shift leading to the tertiary carbocation occurs later along the reaction coordinate; see Figures 4 and 5). In addition, there is considerably less geometric change in going from minimum **3c** to transition-state structure **TS3c→6** in Figure 8 than there is in going from minimum **3c** to transition-state structure **TS3c→5** in Figure 2 (note, for example, that the forming bond distance changes from 3.19 Å to 2.16 Å in the ylangene pathway and from 3.47 Å to 1.94 Å in the sativene/cyclosativene pathway).[53]

(50) The exo and endo deprotonation transition state structures for sativene differ by less than 0.2 kcal/mol (B3LYP/6-31+G(d,p)).

(51) With ammonia as the base, the barrier for deprotonation of **5** (relative to the corresponding reactant complex, **5**···NH_3) to form cyclosativene is approximately 9.9 kcal/mol and the barrier for deprotonation to form sativene is approximately 2.6 kcal/mol (B3LYP/6-31+G(d,p), including unscaled ZPE corrections).

(52) Formation of the ylangenes is related to the formation of the pinenes, camphenes, tricyclene, bergamotenes, and santalene, but we hesitate to draw conclusions about these other terpenes based on our ylangene results due to their structural differences. We will, however, describe calculations on all of these systems in due course.

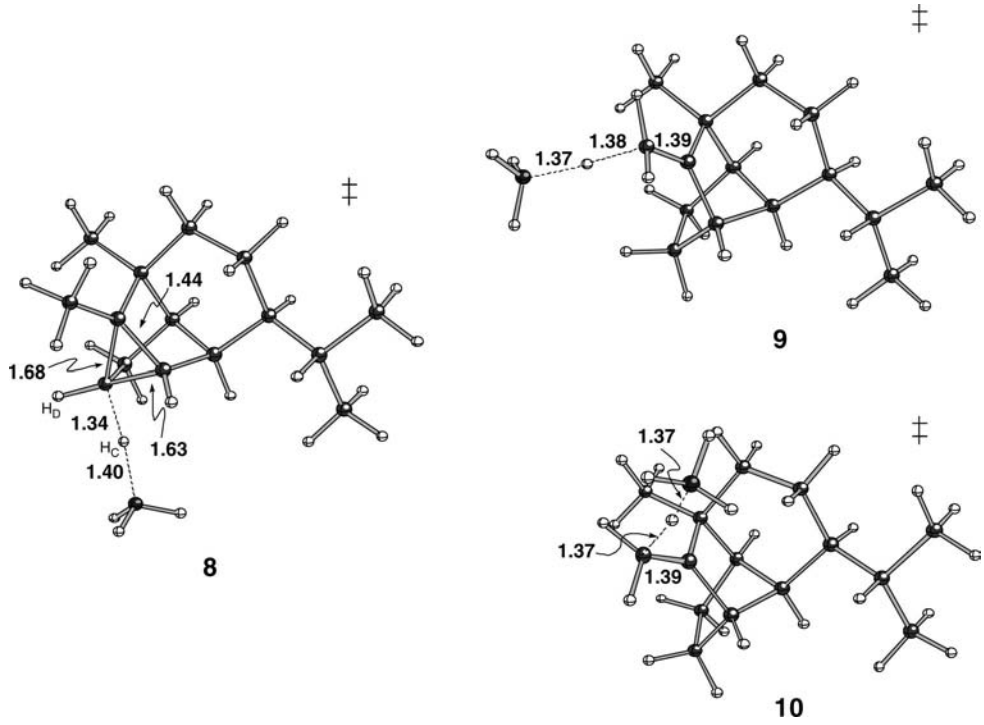

FIGURE 7. Computed deprotonation transition-state structures (using NH_3 as the base) for the conversion of cation **5** to cyclosativene (**8**) and sativene (**9** and **10**) (selected distances in Å).

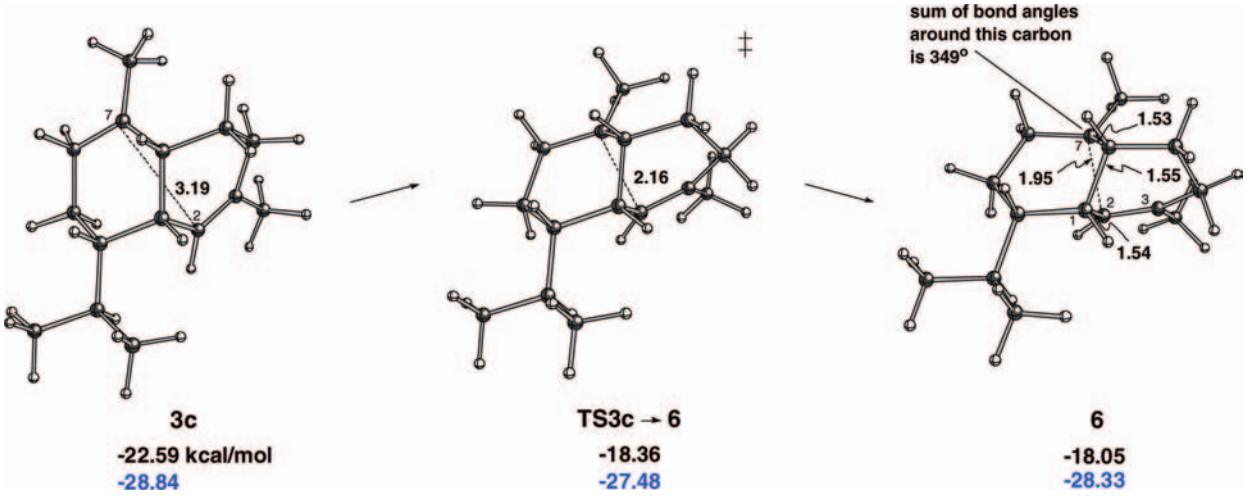

FIGURE 8. Computed geometries and energies (relative to that of **1**) for structures involved in the transformation of **3c** to **6** (the ylangene cation) in Scheme 1. Energies are in kcal/mol; selected distances are in Å. Geometries and energies shown in black are calculated with B3LYP/6-31+G(d,p), energies shown in blue are calculated with mPW1PW91/6-31+G(d,p)//B3LYP/6-31+G(d,p) (zero-point energy corrections from B3LYP calculations are included in the mPW1PW91 energies).

In the forward direction, this transition-state structure is connected to a minimum which is formally a tertiary carbocation adjacent to a four-membered ring (**6** in Scheme 1). As mentioned earlier though, this sort of system might be expected to be unstable with respect to other possibilities, or possibly to display nonclassical ion character.[29–31] Indeed, as shown in Figure 8, the newly formed C−C bond distance in **6** is found to be 1.95 Å. Clearly, this is too long to be considered a full bond, or even a bond that is strongly hyperconjugating to the adjacent cationic center. Although the C1−C2 bond is also adjacent to the carbocationic center (C3), it displays essentially no elongation since it is approximately coplanar with the C3 center, unlike the C2−C7 bond which is approximately perpendicular. Also note that when the B3LYP energies with ZPE corrections are considered, this minimum is actually very slightly higher in energy than **TS3c→6**.[54] The similarity of these energies is likely

(53) It is tempting to correlate the relative barriers for the production of sativene/cyclosativene and the ylangenes to the observed product distribution described in ref 19 (a total of 5.3% and 3.2% respectively). However, these gas-phase barriers do not take into account any effect the enzyme might have on the conformation of the substrate. Additionally, one cannot rule out the possibility that other products arise from diversions after this branch point. Note also that although the barrier to formation of the ylangene cation is smaller than that for the sativene/cyclosativene cation, the overall exothermicity is much less (see Figure 8).

(54) This is a result of the ZPE correction. When the non-ZPE corrected B3LYP energies are considered, the minimum (**6**) is actually lower in energy than the transition structure by 0.07 kcal/mol.

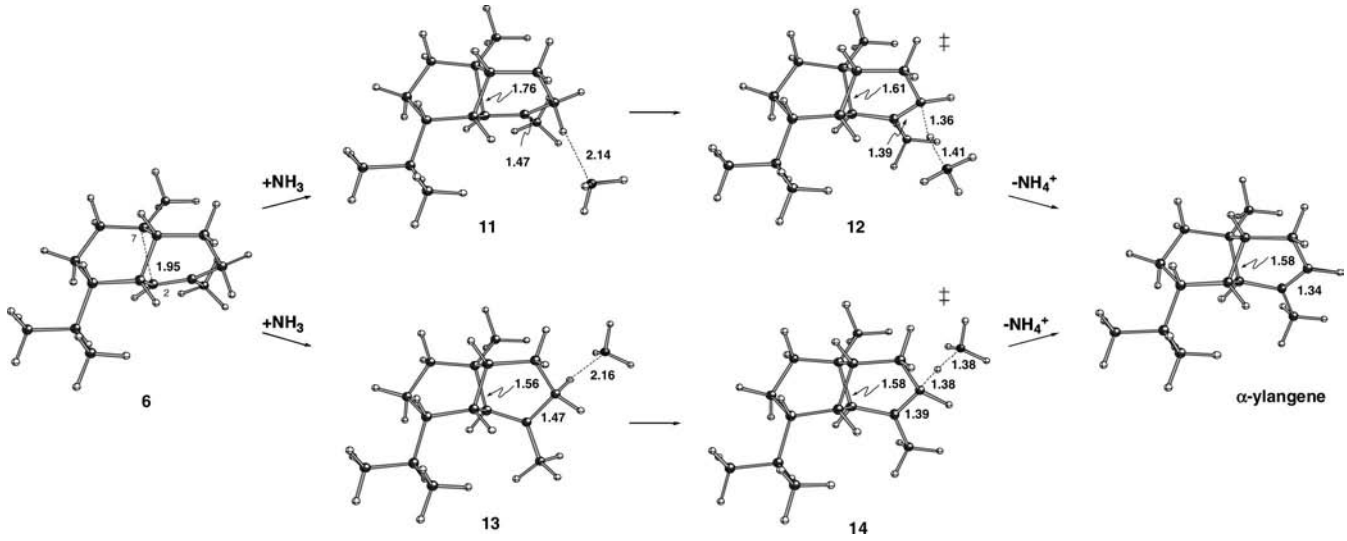

FIGURE 9. Computed structures (B3LYP/6-31+G(d,p), selected distances in Å) showing the progressive decrease in the forming C−C bond distance for α-ylangene. The cation **6** is first shown as complexes with ammonia (**11** and **13**), second in deprotonation transition-state structures (**12** and **14**), and third in the fully deprotonated structure (α-ylangene; here the structure is oriented differently than in Figure 1).

a consequence of an increase in ring strain as the cyclization proceeds; the increased strain effectively cancels out any exothermicity associated with the forming bond and results in a nearly flat potential energy surface. Although the bond is not fully formed, structure **6** is distinct from the other conformers of the 6,6-ring system in that there is clearly some interaction between C7 and C2. It should be noted that structure **6** is, in principle, related to proposed secondary carbocation **4** via a 1,2-alkyl shift (of the C2−C7 "bond"). Attempts to find a transition-state structure that connects **6** to **4** (or possibly **6** to **5** via a concerted, asynchronous reaction similar to that described above for **3** to **5**) were unsuccessful and instead led to the **TS3c→5** transition state structure.[55]

To ascertain whether intermediate **6** can actually lead directly to the two ylangene products, we utilized an approach similar to that described above for cyclosativene. We were able to find minima with the carbocation complexed to ammonia via either of the two hydrogen atoms that would lead to α-ylangene as well as either of the two hydrogen atoms that would lead to *β*-ylangene, and we located transition-state structures for all four corresponding deprotonation steps. These structures for α-ylangene are shown in Figure 9, and the corresponding structures for *β*-ylangene are provided in the Supporting Information. Interestingly, the C−C distance corresponding to the bond that forms when the four-membered ring closes (C2−C7) decreases significantly simply upon complexation with ammonia. This result is consistent with our recent study of the norbornyl cation, where we found that the structure of the nonclassical norbornyl cation is significantly perturbed toward a classical structure upon site-specific complexation with ammonia or benzene.[9] With the exception of the **6 → 13 → 14** pathway,[56] the C2−C7 distance decreases further in the transition state structures, before finally achieving a distance of 1.58 Å in the sesquiterpene product.[57]

As mentioned previously, the branch point leading to the ylangene structures is intermediate **3c**, which is the immediate precursor to **5** in the sativene/cyclosativene pathway (see Figure 2 and Scheme 2). The energy profile of the overall pathway is thus quite similar to that shown in Figure 3, the only difference being the final ring-closing step which has a barrier of 1−4 kcal/mol and results in an overall exothermicity of 18−28 kcal/mol as shown in Figure 8.

Conclusion

We have uncovered viable mechanistic pathways for the formation of the sesquiterpene natural products sativene, cyclosativene, α-ylangene, and *β*-ylangene using quantum chemical methods. For all four products, our calculations predict a potential energy surface that is quite flat, suggesting that once the appropriate nerolidyl cation is formed in the synthase enzyme, the inherent reactivity of the cationic intermediates may allow for generation of the natural products with minimal additional assistance from the enzyme, beyond perhaps some conformational control and control over the site of ultimate deprotonation.

Our computed pathways are largely consistent with the previously proposed mechanisms, with two exceptions: (1) The proposed secondary cation (**4**) in the pathway to sativene and cyclosativene is not found to be a discreet intermediate in our pathway. Instead, the formation of this intermediate is avoided through a concerted reaction that leads directly to a tertiary carbocation (**5**), the same intermediate that is the direct precursor to sativene. This result, together with the transition structure for deprotonation that we found for the formation of cyclosativene from **5** (Figure 7), suggests that only one of the two proposed routes to cyclosativene is likely. Furthermore, we suspect that sesquiterpene synthase enzymes which are found to produce sativene will also likely produce cyclosativene (provided that the enzyme possesses an appropriately located

(55) These attempts included constrained calculations where the C2−C7 and C3−C7 distances were constrained at 2.05 Å each and also where the C2−C7 and C3−C7 distances were constrained to 1.85 Å and 2.00 Å, respectively.

(56) Structure **13** shows significant perturbation from cation **6**; the perturbation is such that the C2−C7 bond is no longer aligned with the empty p-orbital of the carbocationic center. Thus there is essentially no hyperconjugative interaction between the two, and the C2−C7 bond distance is decreased to 1.58 Å. This distance is slightly elongated in going to the corresponding transition-state structure, **14**.

(57) Note also here that **14** is 2.15 kcal/mol higher in energy (B3LYP/6-31+G(d,p)) than **12**.

active site base for this deprotonation). (2) The cyclobutyl-substituted carbocation proposed in the pathway to the ylangenes is found to exist (in the gas phase) as a shallow minimum in which the four-membered ring is not fully formed. However, we do find that quenching of this carbocationic intermediate via deprotonation can lead to both ylangene structures, which have fully formed cyclobutyl rings. This again is evidence that potentially high energy intermediates such as these can be stabilized sufficiently, without outside assistance from the enzyme, to be viable components of the pathway. Whether or not this potential energy surface changes significantly in the presence of the enzyme remains an open question.

Our theoretical results are also consistent with the experimental observation that H_A (instead of H_B) in structure **1** (Figure 2) migrates to the isopropyl group (either via a 1,3-hydride shift or perhaps through a deprotonation−reprotonation sequence). We also found evidence that copacamphene formation via a crossover from the sativene/cyclosativene pathway is possible, and therefore, the experimental observation that γ-humulene synthase does not produce copacamphene suggests that the enzyme either does not provide selective acceleration of this step or perhaps that the enzyme specifically disfavors this alternative. Finally, there appear to be various stereochemical alternatives for the final deprotonation steps leading to sativene, cyclosativene, and the ylangenes, and, for each system, there does not appear to be an inherent energetic preference for any particular deprotonation pathway. We hope that these results will provide meaningful jumping off points for rational reengineering of the γ-humulene synthase active site to bias the distribution of terpenes produced if a crystal structure should become available.

Acknowledgment. We gratefully acknowledge the University of California, Davis and the National Science Foundation (CAREER program and computer time from the Pittsburgh Supercomputer Center) for support. We thank Young Hong for helpful comments and assistance in finding structure **TS2b→3a**. We also thank the anonymous reviewers for their helpful suggestions.

Supporting Information Available: Coordinates and energies for all structures, IRC plots, full Gaussian03 citation, and a scheme showing the relationship of the pathways described herein to those leading to the cubebenes and copaenes. This material is available free of charge via the Internet at http://pubs.acs.org.

JO800868R